

# Vehicular traffic flow at an intersection with the possibility of turning

M. Ebrahim Foulaadvand<sup>1,2</sup> and Somayyeh Belbasi<sup>1</sup>

<sup>1</sup> *Department of Physics, Zanzan University, P.O. Box 19839-313, Zanzan, Iran. and*

<sup>2</sup> *Computational Physical Sciences Laboratory, Department of Nano-Science, Institute for Research in Fundamental Sciences (IPM), P.O. Box 19395-5531, Tehran, Iran.*

(Dated: January 20, 2013)

We have developed a Nagel-Schreckenberg cellular automata model for describing of vehicular traffic flow at a single intersection. A set of traffic lights operating in fixed-time scheme controls the traffic flow. Open boundary condition is applied to the streets each of which conduct a uni-directional flow. Streets are single-lane and cars can turn upon reaching to the intersection with prescribed probabilities. Extensive Monte Carlo simulations are carried out to find the model flow characteristics. In particular, we investigate the flows dependence on the signalisation parameters, turning probabilities and input rates. It is shown that for each set of parameters, there exist a plateau region inside which the total outflow from the intersection remains almost constant. We also compute total waiting time of vehicles per cycle behind red lights for various control parameters.

## I. INTRODUCTION

Simulation of urban traffic flow has shown to be of prime importance for optimisation and control purposes as the number of vehicles increases continuously and traffic conditions deteriorate. Modelling traffic flow dynamics by cellular automata has constituted the subject of intensive research by statistical physics during the past years [1–3]. Understanding the characteristics of *city traffic* is one of the most essential parts of the traffic research and was an early simulation target for statistical physicists [4–12]. Despite elementary attempts for simulation of perpendicular flows [13–17] the first serious cellular automata describing the flow at a signalised intersection was proposed by authors in [18]. Recently, physicists have notably attempted to simulate traffic flow at intersections and other traffic designations such as roundabouts [19–32]. Further recent progresses include various features such as self-organised controlling of traffic lights and flows in networks [33, 34], the modelling of decision-making at intersections [35], mixture of motorized and non motorized vehicles [36], simulation of traffic flow at T-shaped intersections [37, 38], data collection in city traffic [39], application of fuzzy logic in signalisation of intersections [40], visual simulation of vehicular traffic [41] and dynamic route finding strategy [42]. Vehicular flow at the intersection of two roads can be controlled via two distinctive schemes. In the first scheme, the traffic is controlled without traffic lights [28, 43]. In the second, signalised traffic lights control the flow. In Ref. [18], we have modelled the traffic flow at a single intersection with open boundary conditions applied to the streets. In a recent study, a single intersection operating under fixed time and traffic responsive schemes has been explored with closed boundary condition [44]. In the mentioned papers cars were restricted to move straightly and not allowed to change their directions when they reach to the intersection. In this work we incorporate the possibility of turning. This incorporation constitutes a crucial step for a more realistic description of traffic flow and would certainly help us in a proper coordination of traffic lights.

## II. DESCRIPTION OF THE PROBLEM

Consider the traffic flow at the intersection of two streets. Each street conducts a uni directional flow and has a single lane. Here for simplicity we exclude the possibility of overtaking which requires having more than one lane and some laws for lane-changing [45]. The flow directions are taken south-north in street one and east-west in street two. Vehicles can turn when reaching to the intersection. A northward moving car can turn left and a westward moving car can turn right (towards north) when reaching to the intersection. We model each street by a chain of  $L$  sites. These perpendicular chains intersect each other at the middle sites  $i_1 = i_2 = \frac{L}{2}$  (see Fig.1 for illustration). The discretisation of space is such that each car occupies an integer number of cells denoted by  $N_{cell}$ . Cell length is denoted by  $\Delta x$ . The car position is denoted by the location of its head cell. Time elapses in discrete steps of  $\Delta t$  and velocities take discrete values  $0, 1, 2, \dots, v_{max}$  in which  $v_{max}$  is the maximum velocity measured in unit of  $\frac{\Delta x}{\Delta t}$ . The probability of turning a north-moving car to west is denoted by  $p_{sw}$ . Correspondingly the probability of turning a west-moving car to north is denoted by  $p_{en}$ .

At each step of time, the system is characterized by the position and velocity configurations of cars. The system evolves under the Nagel-Schreckenberg (NS) dynamics [46]. Let us now specify the physical values of our time and space units. The length of each car,  $L_{car}$ , is taken 4.5 metres. Therefore, the spatial grid  $\Delta x$  (cell length) equals to  $\frac{4.5}{N_{cell}}$  m. We take the time step  $\Delta t = 1$  s. Furthermore, we adopt a speed-limit of 74 km/h. In addition, each discrete increment of velocity signifies a value of  $\Delta v = \frac{4.5}{N_{cell}} m/s$  which is also equivalent to the acceleration value. For  $N_{cell} = 5$  we have  $v_{max} = 23$  cells per time step. Moreover, the acceleration takes the comfort value  $a = 0.9 \frac{m}{s^2}$ . The value of random braking parameter is taken  $p = 0.1$  throughout this paper. A set of traffic lights controls the traffic flow in a fixed-time scheme as follows.

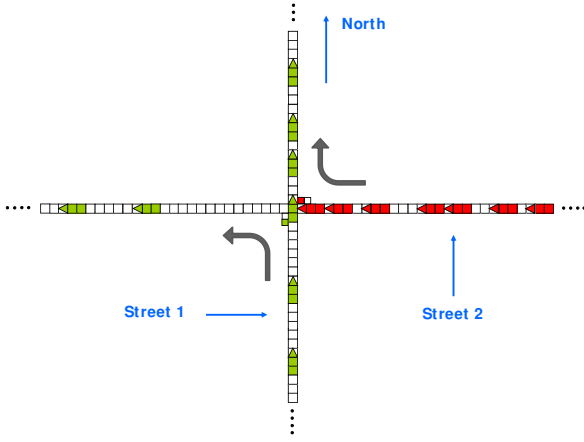


FIG. 1: Intersection of two uni-directional single-lane streets with possibility of car turning at the intersection.

### A. Fixed Time Signalisation of lights

In this scheme the traffic lights periodically turn into red and green. The period  $T$ , hereafter referred to as *cycle time*, is divided into two phases. In the first phase with duration  $T_g$ , the lights are green for the westward street and red for the northward one. In the second phase which lasts for  $T - T_g$  time steps the lights change their colour and become red for the northward and green for the westward street. The gap of all cars are updated with their leader vehicle except the ones (in each street) which are the nearest approaching cars to the intersection. These two cars need special attention. For these cars gap should be adjusted with the signal in its red phase. In this case, the gap is defined as the number of cells immediately after the car's head to the intersection point  $\frac{L}{2}$ . If the head position of the approaching car lies in the crossing point the gap is zero. Note that for  $N_{cell} > 1$  at a time step when a light goes red for a direction, portion of a passing car from that direction can occupy the crossing point. In this case the leading car of the queue in the other direction should wait until the passing car from the crossing point completely passes the intersection i.e.; its tail cell position become larger than  $\frac{L}{2}$ .

### B. Modelling the car turning

To model car turning we proceed as follows: once a car becomes approaching to the intersection we draw a random number  $r$  (uniformly chosen from the unit interval). If  $r$  is less than the corresponding turning probability the car turning label becomes one otherwise it remains zero. In the subsequent time steps the approaching car's gap is adjusted appropriately: if its

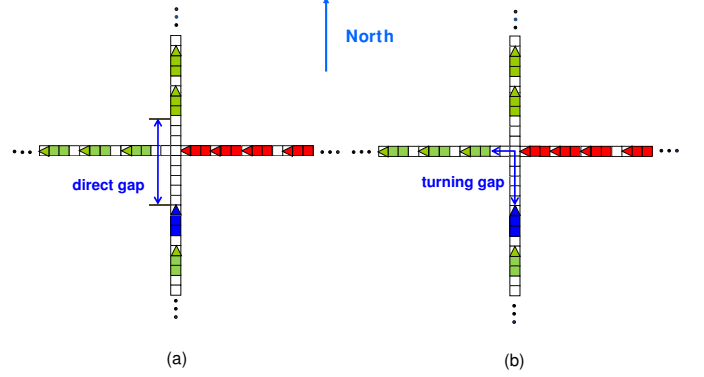


FIG. 2: A turning adjusts its gap to the appropriate front car in the destination lane. (a): the approaching car in street one does not intend to turn. (b): the approaching car in street one intends to turn.

turning label is zero its gap is adjusted via its forward leading car otherwise if its turning label is one the gap is adjusted via the first car in the perpendicular direction which has already passed the intersection (see figure 2).

### C. Entrance/Removal of cars to/from the intersection

The type of boundary condition we implement in this paper is *open*. the reason is that if one tries to imply close type boundary condition, after some time steps most of the cars will appear in that street which has a higher turning probability into it. This effect arises because of accumulation of cars in the street with higher inward turning probability. To avoid such spurious effect which is surely contradicting to what occurs in reality we impose open boundary condition. This type of boundary condition is more compatible to realistic traffic flow. For this purpose, we define two integer-valued parameters  $d_1 \geq 1$  and  $d_2 \geq 1$  for streets one and two respectively.  $d_i$  is inversely proportional to the traffic density in street  $i$ . Once the distance of the nearest car to first chain cell  $j = 1$  (farthest car to the intersection) in street  $i$  ( $i = 1, 2$ ) exceeds  $d_i$  a new car is inserted at site  $j = 1$  of street  $i$  with maximum velocity  $v_{max}$ . The removal of cars from a street is modelled as follows: when the position of a car which has passed the intersection becomes larger than  $L - N_{cell}$  this car is removed from the system and the number of exited cars is increased by one correspondingly. The output current from street  $i$  is defined as the number

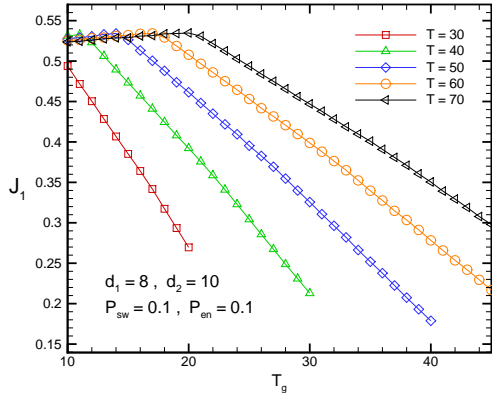


FIG. 3:  $J_1$  versus  $T_g$  at  $v_{max} = 4$  for cycle time  $T = 30, 40, 50, 60$  and  $70$  seconds. The values of other parameters are specified in the figure. Street one has a higher input rate than street two. Turning probabilities are equal to each other.

of cars exited from street  $i$  during a time interval  $[T_1, T_2]$  divided by the  $T_2 - T_1$ . We denote the output currents by  $J_1$  and  $J_2$  for street one and two respectively.

### III. SIMULATION RESULTS

Now all the computational ingredients for simulation is at our disposal. We have taken the streets sizes equal to  $1350 m$ . For  $N_{cell} = 1$  this corresponds to  $L_1 = L_2 = 300$  cells). The system is updated for  $2 \times 10^5$  time steps. After transients, two streets maintain steady-state currents  $J_1$  and  $J_2$  which are defined as the number of vehicles passing the intersection per time step. They are functions of input rates  $\frac{1}{d_1}$  and  $\frac{1}{d_2}$ , turning probabilities  $p_{sw}, p_{en}$  and signal times  $T$  and  $T_g$ .

#### A. $N_{cell} = 1$

In this case, each cell accommodates a car. Figure (3) shows variation of  $J_1$  versus green period of street two (east-west)  $T_g$  for some values of cycle time  $T$ . The maximum of  $J_1$  is less than  $T_g = \frac{T}{2}$  because street two is less loaded than street one. The inequality of input rates makes the slope  $J_1$  different at the vicinity of  $\frac{T}{2}$ . For a given set of parameters, one can maximise the output current of street one by setting  $T_g$  to the maximising value. Sharp fall of  $J_1$  is noticeable and is related to enhancing of jammed region in street one.

Figure (4) depicts the behaviour of  $J_1$  versus  $T_g$  but this time for various values of input parameter  $d_1$ . Other parameters are specified in figure. By decreasing the green time of street one, its output current slightly increases until it reaches to plateau region on which  $J_1$  is

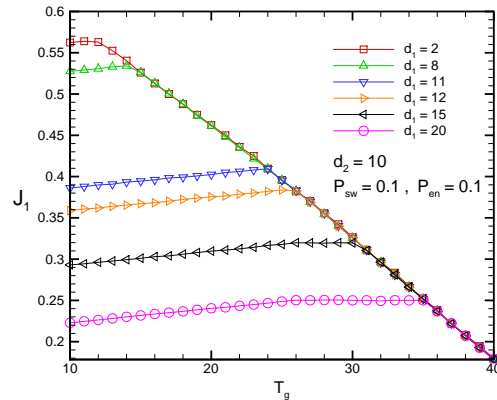


FIG. 4:  $J_1$  vs  $T_g$  for various values of  $d_1$  at  $T = 50$  and  $v_{max} = 4$ . Other parameters values are specified in the figure.

maintained constant. The reason is that the red cycle of light optimally organises the output flow from the intersection. This might be seem counterintuitive to the expectation the less the red period the larger the out flow. However, we should note that turning cars from east-west street contribute to  $J_1$  too.

Figure (5) exhibits  $J_2$  versus the the green time devoted to street two for various values of input rates of street one. Two distinctive behaviour can be identified. For a given  $d_1$  the current  $J_2$  increases by increasing street two green time  $T_g$  up to certain value. Afterwards  $J_2$  remain constant on a small plateau region and start to decrease in a slight manner afterwards. The reason is that by increasing  $T_g$  the green time of street one decreases. This reduces the current of south-west turning car into street two. In fact,  $J_2$  has two sources: straight moving east-west cars in street two and south-west turning cars in street one. Beyond a certain  $T_g$  the contribution of the second source dramatically falls which makes  $J_2$  show a maximum.

Let us now look at the behaviour of the total flow  $J_{tot} = J_1 + J_2$  versus  $T_g$  and  $d_1$ . Figure (6) shows this variation versus street two green time  $T_g$  for various values of cycle time  $T$ . The notable point is that the maximum total flow only weakly depends on the cycle time  $T$ . For each  $T$  there is a plateau region maintaining a maximum flow. This region is centered at a  $T_g = \alpha T$  and increases with cycle time  $T$ .  $\alpha$  depends on the streets input rates and is less than  $0.5$  when  $d_2$  is less than  $d_1$ . Roughly speaking  $\alpha = \frac{d_1}{d_1 + d_2}$ . The slope is symmetrical on both side of the plateau region.

In figure (7)  $J_{tot}$  is sketched versus  $T_g$  this time for various values of street one input rate  $d_1$ . Typically the total flow shows a three-regime behaviour: an increasing, a plateau and eventually a decreasing portion. The plateau length decreases with increase in  $d_1$ . These three portions are associated to the competition of two competing features. The direct current and the turning current.

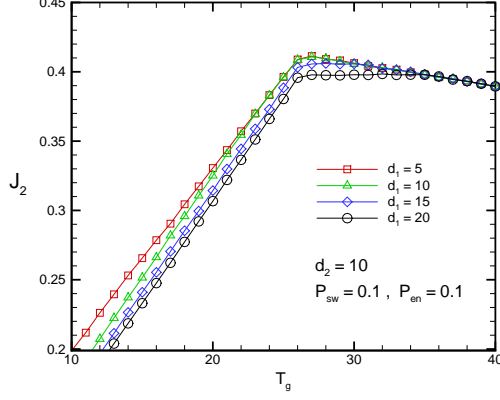


FIG. 5:  $J_2$  vs  $T_g$  of street two for various values of  $d_1$  at  $v_{max} = 4$ . Other parameters values are specified in the figure.

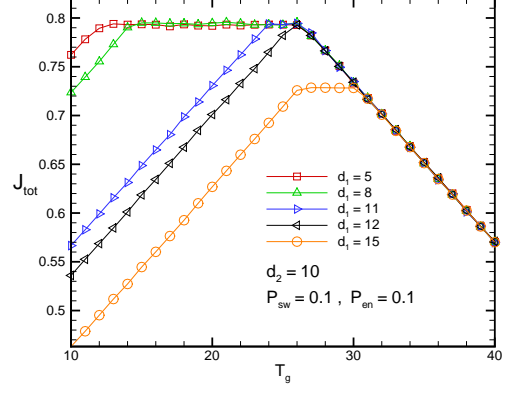


FIG. 7:  $J_{tot}$  vs  $T_g$  for various values of  $d_1$  at  $v_{max} = 4$ . Other parameters values are specified in the figure.

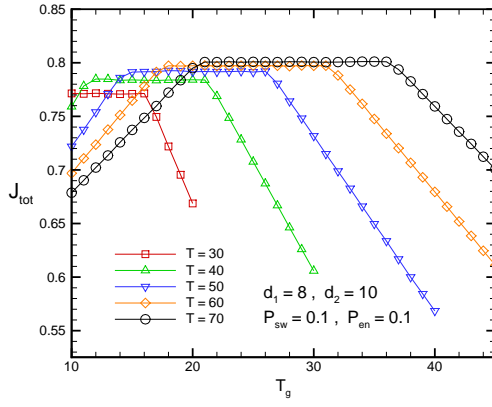


FIG. 6:  $J_{tot}$  vs  $T_g$  of street two for various values of  $T$  at  $v_{max} = 4$ . Other parameters values are specified in the figure.

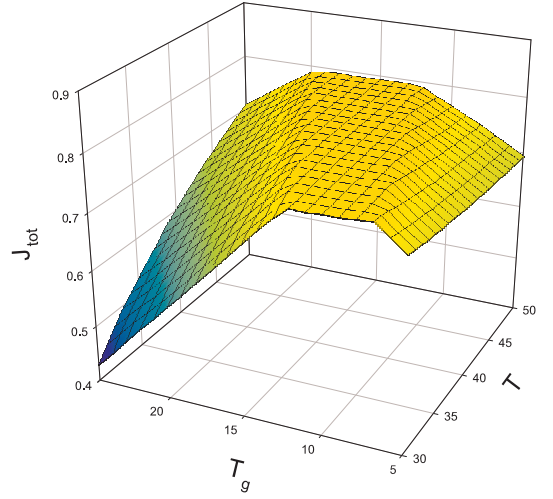


FIG. 8: Three dimensional plot of  $J_{tot}$  vs  $T$  and  $T_g$ .  $d_1 = 7$ ,  $d_2 = 15$ ,  $v_{max} = 4$  and turning probabilities are equally set at 0.1.  $J_{tot}$  retains a constant value on a wide plateau region and sharply falls outside the plateau.

The plateau region corresponds to the situation where two features are balanced and equally contribute to the total current.

To gain a deeper insight into the problem, we have obtained the mutual dependence of the total flow  $J_{tot}$  on input rate parameters  $d_1$  and  $d_2$  for equal turning probability  $P_{sw} = P_{en} = 0.1$  in figure (8) (see the journal printed version). Other parameters are specified in the figure. We see the existence of a two dimensional plateau on which the total flow is maximised. The maximum throughput flow is slightly less than 0.8. Moreover, the total current  $J_{tot}$  is symmetric respect to the plane  $d_1 = d_2$  as it should be. The staircase like topography of the current surface and the appearance of semi plateau regions are noticeable. We see the dramatic fall of the total current in the vicinity of the plane  $d_1 = d_2$ . This marks the inefficiency of the fixed-time scheme in organising the flow via equal distribution of cycle times to equally loaded streets. In figures (9) (see the journal

printed version) and (10) we have sketched the  $J_{tot}$  versus  $T$  and  $T_g$  for given input rates. As you can see there is a relative large plateau on which the total current is maximal. The shape, size and orientation of this plateau show strong dependence on input rates  $d_1$  and  $d_2$ . The maximal current value poorly depends on input rates.

Dependence of  $J_{tot}$  on turning probabilities could serve us to achieve a better understanding from the overall flow characteristics of our single intersection. Figure (11) exhibits such behaviour (see the journal printed version). The current surface has interesting properties. There is a wide plateau region maintaining a large current between 0.8 and 0.85. Sharp decrease is followed when  $|p_{sw} - p_{en}|$  becomes large. To see the reason consider a situation where  $p_{sw}$  is large whereas  $p_{sw}$  is small. Therefore most

of the entrant cars to street two move straight forward to west. On the other hand most of the entrant cars to street one prefer to turn left (towards west) when reaching to the intersection. This causes a dramatic jam in the vicinity of the intersection which leads to a sharp decrease of the total current. In figure (12) (see the journal printed version) we have depicted a similar 3D plot this times for unequal input rates  $d_1 \neq d_2$ . Other parameters are identical to those in figure (11). The prominent effect of having unequal input rates is the reduction of the maximal current value in the plateau region from 0.82 roughly to 0.71. Other characteristics are analogous to the case  $d_1 = d_2$ . Comparison of figure (10) and (11) suggests that fixed-time signalisation can poorly adjust itself to variation of turning probabilities and implementation of more efficient adaptive strategies is inevitable.

### Waiting times:

Despite maximising the output currents is highly desirable for us but it may not be the ultimate task in optimisation of traffic flow. Another important parameter for optimisation of the traffic flow at intersections are aggregate waiting times of cars stopping at queues formed in the red cycle of the traffic lights. In our model this total waiting time, denoted by  $WT_{tot}$  onwards, can be simply be evaluated. Once a car reaches to the end of a queue the  $WT_{tot}$  counter is increased by one at each time step. This counting is paused once the corresponding light goes green. In figure (13) we show the  $WT_{tot}$  per cycle versus green time of street two for various values of cycle time  $T$ . The system has evolved for  $10^5$  timesteps. The first 20000 timestep has been discarded for equilibration. Contrary to total current dependence on  $T_g$ , here we do not have a minimal plateau region but rather there exists a global minimum for  $WT_{tot}$ . This is helpful to us in achieving the optimisation of traffic light by simultaneous maximising the total current and minimisation of total waiting time. The results of figure (13) and (6) suggest to take the  $T_g$  at the end of current maximal plateau as the optimal choice for the green time distribution.

To gain a deeper insight, we have drawn a 3D plot of the  $WT_{tot}$  versus various control parameters in figures (14) and (16). In figure (14) (see the journal printed version) the mutual dependence of  $WT_{tot}$  on input rates  $d_1$  and  $d_2$  for  $T = 30$  and  $T_g = 15$  is plotted. The qualitative topography of the  $WT_{tot}$  surface resembles much with figure (8). For both  $d_1$  and  $d_2$  larger than 13 (light traffic in both streets) we have a relatively small  $WT_{tot}$ . Once either of  $d_1$  or  $d_2$  becomes less than 11 a dramatic increase in  $WT_{tot}$  is observed. Figure (15) sheds more light onto the problem. This figure is a 2D view of figure (14) and clearly shows the staircase-like structure of  $WT_{tot}$  surface. The sharp fall of  $WT_{tot}$  is noticeable. In figure (16) (see the journal printed version) total waiting time per cycle is mutually sketched versus turning probabilities for fixed equal input rates. We see there is a wide minimal plateau on which the total waiting time

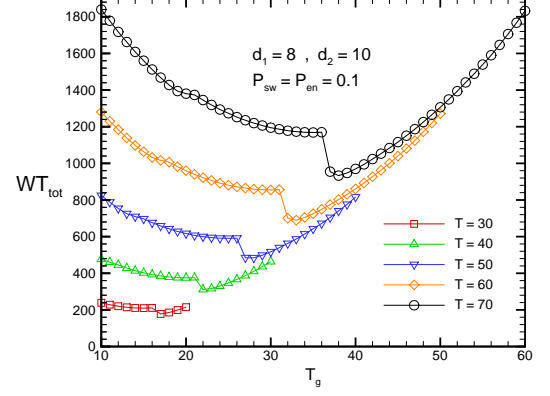


FIG. 9: Total waiting time per cycle vs  $T_g$ . Street one accommodates a heavier traffic flow ( $d_1 = 8, d_2 = 10$ ).  $v_{max} = 4$  and turning probabilities are equally taken 0.1.

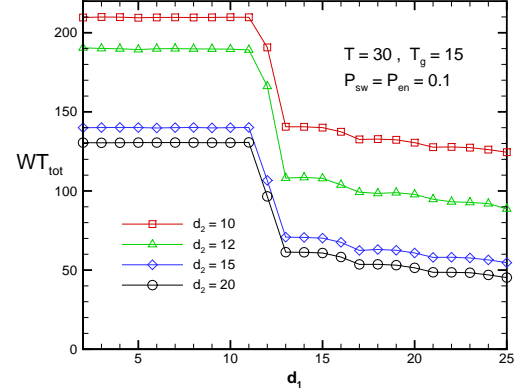


FIG. 10: Dependence of  $WT_{tot}$  per cycle on  $d_1$  for fixed values of  $d_2$ . Other parameters:  $v_{max} = 4$ ,  $T = 30$ ,  $T_g = 15$  and turning probabilities are equally taken 0.1.

retains its constant minimal value. On the boundaries where  $|p_{sw} - p_{en}|$  becomes large the waiting time dramatically begins to increase. The behaviours of total current and total waiting times are complementary to each other i.e.; the maximum of  $J_{tot}$  coincides with the minimum of  $WT_{tot}$ . It is our expectation that such complimentary between  $WT_{tot}$  and  $J_{tot}$  remains valid for the cases in which the input rates are not equal.

We end this section by showing 3D plots of  $WT_{tot}$  mutually versus  $T$  and  $T_g$ . In figure (17) (see the journal printed version)  $WT_{tot}$  is given for  $d_1 = d_2 = 8$ . There is no minimal plateau sharply separated from high values. The curve is very smooth and low value region gently crosses over to high values of waiting times. When considering non equal input rates, the situation becomes worse. In figure (18) (see the journal printed version) the  $WT_{tot}$  is sketched for  $d_1 = 7 \neq d_2 = 15$ . Once again we see the region of maximal total current does not

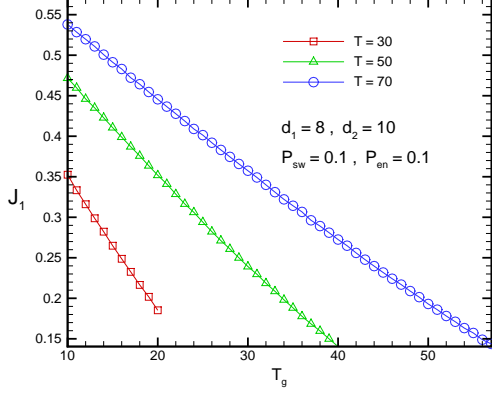


FIG. 11:  $J_1$  vs  $T_g$  at  $v_{max} = 23$  for  $N_{cell} = 5$ . The values of other parameters are identical to figure (3).

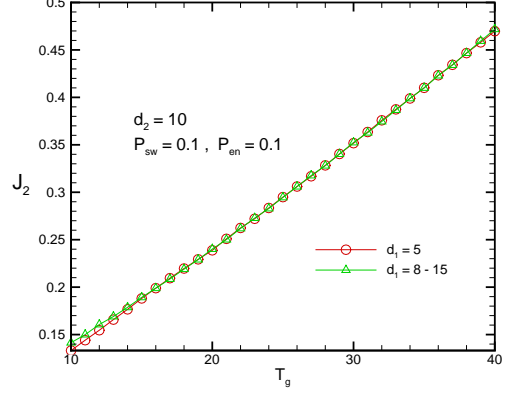


FIG. 13:  $J_2$  vs  $T_g$  of street two for various values of  $d_1$  at  $N_{cell} = 5$ .  $v_{max} = 23$ . Other parameters values are identical to figure (5).

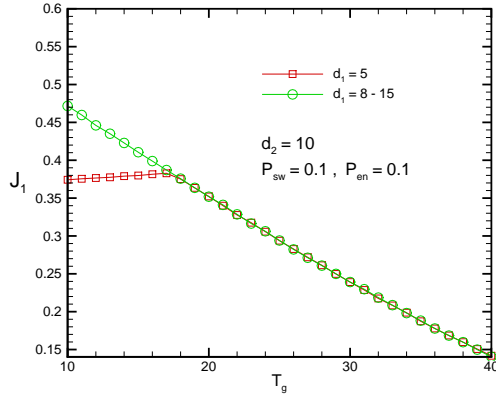


FIG. 12:  $J_1$  vs  $T_g$  for various values of  $d_1$  with  $N_{cell} = 5$ . Other parameters values are identical to figure (19).

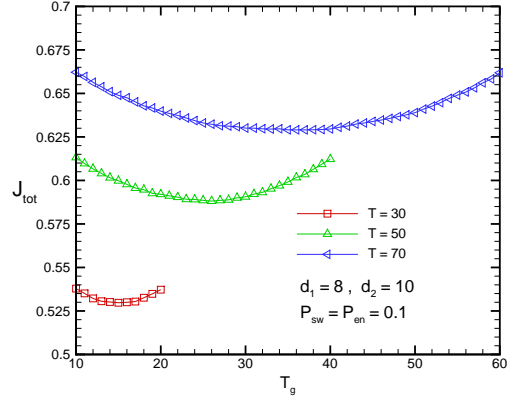


FIG. 14:  $J_{tot}$  vs  $T_g$  of street two for various values of  $T$  at  $N_{cell} = 5$ . Other parameters values are identical to figure (6).

entirely overlap with the region of minimal waiting time. This demonstrates the optimisation of traffic flow is not a simple task at least within the framework of NS model. Obviously empirical data is needed and can illuminate the problem.

### B. $N_{cell} = 5$

In this section we show the results for a multi-cell occupation of cars. Here we take  $N_{cell} = 5$  as discussed in section II. In this case we have the comfort acceleration  $a = 0.9 \text{ m/s}^2$ . We have reproduced figures 3-7 to see the similarities/differences imposed by varying  $N_{cell}$ . Figures (19-20) show exactly the same graphs as in figures (3-4). The only difference is due to  $N_{cell}$  which is now equal to 5.

The most prominent difference is that in  $N_{cell} = 5$  the current  $J_1$  is decreasing whereas in  $N_{cell} = 1$  it slightly

increases with  $T_g$  and then starts to decrease. Currents  $J_1$  in uni-cell i.e.,  $N_{cell} = 1$  are in general larger than their counterparts in multi-cell case. This is due to unrealistic large acceleration in the NS model for uni-cell occupation. Figure (21) sketches the same diagram shown in figure (5) for  $N_{cell} = 5$ . As you see  $J_2$  is an increasing function of  $T_g$  while in uni-cell case it reaches to a maximum, then after a short plateau it declines.

Figures (22) and (23) exhibit dependence of total current  $J_{tot}$  versus  $T_g$  for various values of cycle time  $T$  and input rate  $d_1$ .

Here also we encounter substantial differences. The most distinguishable feature is the convex nature of total waiting time curve. In sharp contrast to uni-cell case, in multi-cell occupation, we do not have a plateau region. Instead a smooth decrease is observed up to a minimum and then it symmetrically begins to increase. Analogously, the total current value is less than the uni-cell



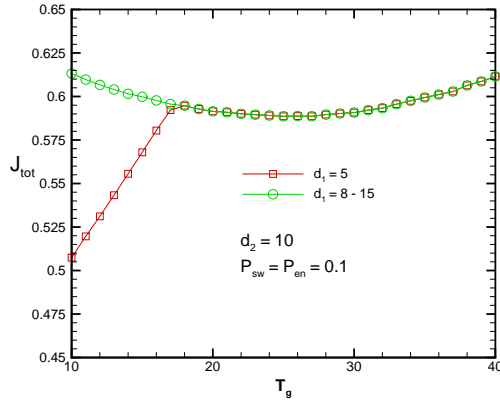


FIG. 15:  $J_{tot}$  vs  $T_g$  for various values of  $d_1$  at  $N_{cell} = 5$ .

due to the same reason explained for  $J_1$  and  $J_2$ . In figure (23) and for  $d_1 = 5$  The behaviour for small  $T_g$  is similar to uni-cell case i.e.;  $J_{tot}$  increases. The difference is that in uni-cell it reaches to a maximum and then increase sharply whereas in multi-cell occupation  $J_{tot}$  does not decrease after linear increasing regime is ended. For  $d_1 > 5$  we do not have the increasing behaviour for small  $T_g$ .

#### IV. SUMMARY AND CONCLUDING REMARKS

In summary, we have simulated the vehicular traffic flow at a single intersection in which the possibility of turning when cars reach to the intersection is augmented to the problem. A set of traffic lights operating in a fixed time scheme controls the flow. We have tried to shed some light onto the problem of traffic optimisation by extensive simulations. Total current is shown to remain constant on a plateau of green time period given to one

of the directions. Three dimensional plot of total current for given input rates of vehicles in terms of signalisation parameters shows the existence of a 2D plateau region encompassed by almost flat planes of sharp decreasing currents. By extensive simulations we have examined the effect of turning on the output current. The dependence of  $J_{tot}$  on the whole range of turning probabilities for fixed values of other parameters have been computed including the equal and nonequal input rates. The main finding is the appearance of a plateau current associated the central region of the  $P_{sw} - P_{en}$  plane. The current sharply decreases when  $|P_{sw} - P_{en}|$  becomes large. Needless to say the plateau characteristics i.e.; its size and height depend on the input rate and signalisation parameters  $T$  and  $T_g$ . Similar properties is observed if instead of  $J_{tot}$  one looks at total waiting time per cycle. Note here the waiting times sharply increase when  $|P_{sw} - P_{en}|$  becomes large. Besides total current, total waiting time per cycle has been computed. Our investigations reveal that in the parameter space, the minimisation of total waiting time per cycle does not fully coincide with the maximisation of total current. This arises the natural question of *what quantity should be optimised in order to acquire the most efficiency for the intersection ?* In our Nagel-Schreckenberg cellular automata, not only the case of uni-cell occupation, where each cell accommodates a car, has been considered but also the more realistic case of multi cell occupation in which a car occupies more than one cell has been investigated. The corresponding results differ quantitatively and in some case qualitatively. Seeking for advanced models properly designated for modelling the behaviours of drivers at intersections is inevitable and unavoidable. We would like to end by emphasizing on the role of empirical data for adjusting the parameters of any intersection traffic model. Despite utilising multi-cell occupation can render the deceleration/acceleration value of moving cars to a realist one, the behaviour of halted cars in the queue when the light goes green is still suffering from a satisfactory modelling.

- 
- [1] D. Chowdhury, L. Santen and A. Schadschneider, *Physics Reports*, **329**, 199 (2000).
  - [2] D. Helbing, *Rev. Mod. Phys.*, **73**, 1067 (2001).
  - [3] C. Appert-Rolland, F. Chevier, P. Godret, S. Lasarre, J-P. Lebacque and M. Schreckenberg (eds.) *Traffic and Granular flow 07*, (Springer, 2009).
  - [4] O. Biham, A. Middleton and D. Levine, *Phys. Rev. A*, **46**, R6124 (1992).
  - [5] J.A. Cuesta, F.C. Martinez, J.M. Molera and A. Sanchez, *Phys. Rev. E*, **48**, R4175 (1993).
  - [6] T. Nagatani, *J. Phys. Soc. Japan*, **63**, 1228 (1994); *J. Phys. Soc. Japan*, **64**, 1421 (1995).
  - [7] J. Freund and T. Pöschel, *Physica A*, **219**, 95 (1995).
  - [8] B. Chopard, P.O. Luthi and P.A. Queloz *J. Phys. A*, **29**, 2325 (1996).
  - [9] S. Tadaki, *Phys. Rev. E*, **54**, 2409 (1996); *J. Phys. Soc. Jpn.* **66**, 514 (1997).
  - [10] J. Török and J. Kertesz, *Physica A*, **231**, 515 (1996).
  - [11] D. Chowdhury and A. Schadschneider, *Phys. Rev. E*, **59**, R 1311 (1999).
  - [12] E. Brockfeld, R. Barlovic, A. Schadschneider and M. Schreckenberg, *Phys. Rev. E*, **64**, 056132 (2001).
  - [13] T. Nagatani, *J. Phys. A*, **26**, 6625 (1993).
  - [14] Y. Ishibashi and M. Fukui, *J. Phys. Soc. Japan*, **65**, 2793 (1996).
  - [15] Y. Ishibashi and M. Fukui, *J. Phys. Soc. Japan*, **70**, 2793 (2001); *J. Phys. Soc. Japan*, **70**, 3747 (2001).
  - [16] M.E. Fouladvand and M. Nematollahi, *Eur. Phys. J. B*, **22**, 395 (2001).
  - [17] M. Krabalek and P. Seba, *J. Phys. A*, **36**, L7 (2003).
  - [18] M. E. Fouladvand, Z. Sadjadi and M. R. Shaebani *J. Phys. A: Math. Gen.*, **37**, 561 (2004).

- [19] M. E. Fouladvand, Z. Sadjadi and M. R. Shaebani *Phys. Rev. E*, **70**, 046132 (2004).
- [20] M. E. Fouladvand, M. R. Shaebani and Z. Sadjadi *J. Phys. Soc. Japan*, **73**, No. 11, 3209 (2004).
- [21] S. Lämmer, H. Kori, K. Peters and D. Helbing, *Physica A*, **363**, 39 (2006).
- [22] R. Jiang, D. Helbing, P. Kumar Shukla and Q-S Wu; *Physica A*, **368**, issue 2, 567 (2006).
- [23] B. Ray and S. N. Bhattacharyya, *Phys. Rev. E*, **73**, 036101 (2006).
- [24] R. X. Chen, K. Z. Bai and M. R. Liu, *Chinese Physics*, **15**, Issue 7, 1471 (2006).
- [25] R. Wang, M. Liu, R. Kemp and M. Zhou, *Int. J. Mod. Phys. C*, **18**, issue 5, 903 (2007).
- [26] D. W. Huang, *Physica A*, **383**, Issue 2, 603 (2007).
- [27] M. Najem, *Int. J. Mod. Phys. C*, **18**, Issue 6, 1047 (2007); *Int. J. Mod. Phys. C*, **19**, Issue 6, 947 (2008).
- [28] M. E. Fouladvand and S. Belbasi, *J. Phys. A: Math. Theor.*, **40**, 8289 (2007).
- [29] A.C. Soh, M. Khalid, M. H. Marhaban and R. Yusof, *Simulation Modelling Practice and Theory*, **17**, Issue: 6, 1081 (2009).
- [30] K-Z Bai, R-X Chen, M-R Liu, L-J Kong and R-S Zheng, *Acta Physica Sinica*, **58**, Issue: 7, 4500 (2009).
- [31] K-Z Bai, H-L Tan, L-J Kong and M-R Liu, *Chinese Physics B*, **19**, Issue: 4, Article Number: 040510 (2010).
- [32] H-F Du, Y-M Yuan, M-B Hu, R. Wang, R. Jiang and Q-S Wu *J. Stat. Mech. : Theory and Experiment*, Article Number: P03014 (2010).
- [33] S. Lammer and D. Helbing, *J. Stat. Mech. : Theory and Experiment*, Article Number: P04019 (2008).
- [34] A. Mazloumian and D. Helbing, *Eur. Phys. Journal B*, **70**, Issue: 2, 257 (2009).
- [35] M. Fukui, K. Nishinari, Y. Yokoya and Y. Ishibashi, *Physica A.*, **388**, Issue 7, 1207 (2009).
- [36] D-F. Xie, Z-Y Gao, X-M Zhao and K-P Li, *Physica A.*, **388**, Issue 10, 2041 (2009).
- [37] X-G Li, Z-Y Gao, B. Jia and X-M Zhao, *Intl. J. of Mod. Physics C*, **20** Issue 4, 501 (2009).
- [38] Z.J. Ding, X.Y. Sun, R.R. Liu, Q.M. Wang and B.H. Wang, *Intl. J. of Mod. Physics C*, **21** Issue 3, 443 (2010).
- [39] G. Seo, A. Yazici, U. Ozguner and J. Cho, *10TH Intl. Conference on Advanced Communication Technology*, Vols I-III, 667 (2008).
- [40] B.M. Nair and J. Cai, *IEEE Intelligent Vehicles Symposium*, Vols 1-3, 147 (2007).
- [41] O. Hatzi, S. Thomas, V. Dalakas, M. Nikolaidou and D. Anagnostopoulos, *Proceeding of European Simulation and Modelling Conference*, 296 (2007).
- [42] J. Fang, J. Shi, X-Q Chen and Z. Qin, *Intl. J. of Mod. Physics C*, **21** Issue 2, 221 (2010).
- [43] M. E. Fouladvand and M. Neek Amal, *Euro. Phys. Lett.*, **80**, issue 6, Article number 6002 (2007).
- [44] M. E. Fouladvand and S. Belbasi, *J. Stat. Mech*, P07021, (2008).
- [45] M. E. Fouladvand, *Phys. Rev. E*, **62**, 5940, (2000),
- [46] K. Nagel, M. Schreckenberg, *J.Phys. I France*, **2**, 2221 (1992).



